Available online at www.sciencedirect.com
ScienceDirect
International Journal of Heat and Fluid Flow 28 (2007) 1492–1506
International Journal of HEAT AND FLUID FLOW
www.elsevier.com/locate/ijhff

Temperature and particle-size dependent viscosity data for water-based nanofluids – Hysteresis phenomenon

C.T. Nguyen [a,*], F. Desgranges [b], G. Roy [a], N. Galanis [c], T. Maré [d], S. Boucher [a], H. Angue Mintsa [a]

[a] Faculty of Engineering, Université de Moncton, Moncton, New Brunswick, Canada E1A 3E9
[b] Institut Supérieur de Technologie Midi-Pyrénées, 31300 Toulouse, France
[c] Faculty of Engineering, Université de Sherbrooke, Sherbrooke, Québec, Canada J1K 2R1
[d] LGCGM, INSA de Rennes/IUT Saint-Malo, Saint-Malo, France

Received 12 June 2006; received in revised form 12 February 2007; accepted 13 February 2007
Available online 6 April 2007

Abstract

In the present paper, we have investigated experimentally the influence of both the temperature and the particle size on the dynamic viscosities of two particular water-based nanofluids, namely water–Al_2O_3 and water–CuO mixtures. The measurement of nanofluid dynamic viscosities was accomplished using a 'piston-type' calibrated viscometer based on the Couette flow inside a cylindrical measurement chamber. Data were collected for temperatures ranging from ambient to 75 °C, for water–Al_2O_3 mixtures with two different particle diameters, 36 nm and 47 nm, as well as for water–CuO nanofluid with 29 nm particle size. The results show that for particle volume fractions lower than 4%, viscosities corresponding to 36 nm and 47 nm particle-size alumina–water nanofluids are approximately identical. For higher particle fractions, viscosities of 47 nm particle-size are clearly higher than those of 36 nm size. Viscosities corresponding to water-oxide copper are the highest among the nanofluids tested. The temperature effect has been investigated thoroughly. A more complete viscosity data base is presented for the three nanofluids considered, with several experimental correlations proposed for low particle volume fractions. It has been found that the application of Einstein's formula and those derived from the linear fluid theory seems not to be appropriate for nanofluids. The hysteresis phenomenon on viscosity measurement, which is believed to be the first observed for nanofluids, has raised serious concerns regarding the use of nanofluids for heat transfer enhancement purposes.

Keywords: Nanofluid; Nanoparticles; Dynamic viscosity; Experimental data; Alumina–water nanofluid; Copper oxide–water nanofluid

1. Introduction

Nanofluids, two-phase mixtures composed of very fine particles in suspension in a continuous and saturated liquid (water, ethylene glycol, engine oil), may constitute a very interesting alternative for advanced thermal applications (Lee and Choi, 1996; Chein and Huang, 2005). It has been found that important heat transfer enhancement may be achieved by using nanofluids instead of conventional fluids; furthermore, some oxide nanoparticles exhibit excellent dispersion properties in traditional cooling liquids. In spite of their remarkable features, few results on nanofluids use in confined flow situations have been published (see Daungthongsuk and Wongwises (2007) for a partial review). Pak and Cho (1998) and Li and Xuan (2002) provided the first empirical correlation for computing Nusselt numbers in laminar and turbulent tube flows using water-based nanofluids. Others have considered the use of nanofluids in microchannel heat sinks (Chein and Huang, 2005). Recent publications (Ben Mansour et al., 2006; Maïga et al., 2005, 2006; Palm et al., 2004 and Roy et al., 2006a) confirmed the heat transfer enhancement due to nanofluids in tube flow and in radial flow between heated disks.

* Corresponding author. Tel.: +1 (506) 858 4347; fax: +1 (506) 858 4082.
E-mail address: Cong.Tam.Nguyen@umoncton.ca (C.T. Nguyen).

0142-727X/$ - see front matter © 2007 Elsevier Inc. All rights reserved.
doi:10.1016/j.ijheatfluidflow.2007.02.004

Nomenclature

T	temperature (°C)
d_p	particle average diameter
h	inter-particle spacing
Greek symbols	
μ	dynamic viscosity (cP)
μ_r	relative viscosity (ratio of nanofluid-to-water viscosities)
φ	volume concentration of particles
φ_m	maximum particle volume fraction
Subscripts	
bf	base fluid (distilled water)
nf	nanofluid
p	particles
r	'nanofluid/ base fluid' ratio

Research efforts have mostly been concerned with the characterization of thermal and physical properties of nanofluids; a good proportion of published studies is of an experimental nature and focuses on the determination of effective thermal conductivities. A review of relevant literature (see in particular Eastman et al., 2004; Murshed et al., 2005; Roy et al., 2006b) has shown an important data dispersion for thermal conductivity obtained from various sources. Furthermore, these data were concerned only with low particle concentrations below 5% in volume. The data dispersion mentioned above may be attributed to various factors such as measuring techniques, particle size and shape, as well as particle clustering and sedimentation. In spite of this, it is clear that the thermal properties of nanofluids are considerably higher than those of the 'conventional' base fluids (Wang et al., 1999; Eastman et al., 1999, 2001). Apart from the pioneering works by Masuda et al. (1993), other relevant and important published results for nanofluid thermal conductivities include those by Choi (1995), Pak and Cho (1998), Lee et al. (1999), Xuan and Li (2000), Murshed et al. (2005) and Liu et al. (2006). Some of the researchers also considered the effect of particle aggregation and interfacial nanolayer (Xuan et al., 2003; Xie et al., 2005). It should be mentioned that there exist, so far, very limited data concerning the temperature effect on nanofluid thermal conductivities (Masuda et al., 1993; Das et al., 2003; Putra et al., 2003). Although the significant dependence of nanofluid thermal conductivity on temperature has clearly been shown, the amount of data remains very limited. The present authors have recently attempted to measure thermal conductivities for alumina–water nanofluids with particle concentrations ranging from 1% to nearly 9% (Roy et al., 2006b). Regarding the modeling of nanofluid effective thermal conductivity, one should mention the recent and interesting models proposed by Koo and Kleinstreuer (2005) and Chon et al. (2005), taking into account effects due to both temperature and particle size. It is worth noting that the differences in modeling nanofluid properties can lead to contradictory results regarding the thermal performance of nanofluids (Ben Mansour et al., 2007; Polidori et al., in press).

Regarding the nanofluid viscosity, the lack of data in the literature is even more striking. Masuda et al. (1993) were likely the first to measure the viscosity of several water-based nanofluids for temperatures ranging from room condition to 67 °C. Pak and Cho (1998) followed with viscosity data obtained for Al_2O_3–water nanofluid and two particle concentrations. Wang et al. (1999) obtained, using three different preparation methods, some data for Al_2O_3–water and Al_2O_3–ethylene glycol mixtures at ambient temperature. Putra et al. (2003) have also provided results showing the temperature effect on Al_2O_3–water nanofluid viscosity for two particle concentrations, namely 1% and 4%. Most recently, Maré et al. (2006), using a Brookfield viscometer with rotating cylinder, obtained some new temperature-dependent viscosity data for Al_2O_3–water at relatively high particle concentrations. To our knowledge, there exist no other data regarding nanofluids dynamic viscosity, a property of crucial importance for all thermal applications involving fluids.

In this paper, we present extensive measurements of the dynamic viscosities for three different water-based nanofluids, Al_2O_3–water with 36 nm and 47 nm particles, and CuO–water with 29 nm particles, for temperatures varying from room conditions to almost 75 °C.

2. Estimation of nanofluid viscosities

From the theoretical point of view, a nanofluid represents a fascinating new challenge to researchers in fluid dynamics and heat transfer because of the fact that it appears very difficult, if not practically impossible, to formulate any theory that can reasonably predict behaviours of a nanofluid by considering it as a multi-component fluid (Xuan and Roetzel, 2000). Yet, since a nanofluid is a two-phase fluid, one may expect that it would have common features with solid–fluid mixtures. The question regarding the applicability as well as the limitations of the classical two-phase fluid theory for use with nanofluids remains unanswered.

There exist few theoretical formulas that can be used to estimate particle suspension viscosities. Almost all such formulas have been derived from the pioneering work of Einstein (1906) which is based on the assumption of a linearly viscous fluid containing dilute, suspended, spherical particles. In that article Einstein calculated the energy dis-

sipated by the fluid flow around a single particle, and associating that with the work required to move this particle relatively to the surrounding fluid, he obtained:

$$\mu_r = \frac{\mu_{nf}}{\mu_{bf}} = 1 + 2.5\varphi \tag{1}$$

Einstein's formula was found to be valid for relatively low particle volume fractions, $\varphi \leqslant 0.02$. Beyond this value, it underestimates the effective viscosity of the resulting mixture. Since the publication of Einstein's work, many articles have been devoted to the 'correction' of his formula. In most of these works, the authors have considered negligible inertial effect in the fluid based on the assumption of a very slow flow, which, in consequence, renders the equations of motion linear. Two factors were often used to 'correct' Einstein's result: the first is that the particles may not be small, and the second is that the structure of the particles within the continuous phase may also affect the viscosity of the mixture. A brief review of the relevant works is given below. Brinkman (1952) has extended Einstein's formula for use with moderate particle concentrations, as follows:

$$\frac{\mu_{nf}}{\mu_{bf}} = \frac{1}{(1-\varphi)^{2.5}} \tag{2}$$

One may also cite the following formula proposed by Frankel and Acrivos (1967):

$$\frac{\mu_{nf}}{\mu_{bf}} = \frac{9}{8} \cdot \left[\frac{(\varphi/\varphi_m)^{1/3}}{1-(\varphi/\varphi_m)^{1/3}} \right] \tag{3}$$

where φ_m is the maximum particle volume fraction as determined experimentally.

On the other hand, Lundgren (1972) has proposed the following equation under the form of a Taylor series in φ:

$$\frac{\mu_{nf}}{\mu_{bf}} = 1 + 2.5\varphi + \frac{25}{4}\varphi^2 + O(\varphi^3) \tag{4}$$

It is obvious that if the terms $O(\varphi^2)$ or higher are neglected, the above formula reduces to that of Einstein.

Batchelor (1977), in his theoretical analysis, considered the effect due to the Brownian motion of particles on the bulk stress of an approximately isotropic suspension of rigid and spherical particles. He proposed the following formula:

$$\frac{\mu_{nf}}{\mu_{bf}} = 1 + 2.5\varphi + 6.5\varphi^2 \tag{5}$$

Graham (1981) has proposed a generalized form of the Frankel and Acrivos (1967) formula that agrees well with Einstein's for small φ. Graham (1981) formula is:

$$\frac{\mu_{nf}}{\mu_{bf}} = 1 + 2.5\varphi + 4.5 \left[\frac{1}{\left(\frac{h}{d_p}\right) \cdot \left(2 + \frac{h}{d_p}\right) \cdot \left(1 + \frac{h}{d_p}\right)^2} \right] \tag{6}$$

where d_p is the particle radius and h is the inter-particle spacing.

From the above formulas, it is apparent that the effective viscosity of a viscous fluid containing suspended solid particles is a function only of the fluid viscosity and particle volume fraction. In principle, all these formulas may also be used for the determination of the viscosity of a nanoparticle suspension. The limitations and validity of such an application remain, however, highly questionable. Brinkman's formula in particular, which was adopted in various studies considering nanofluids (Chein and Huang, 2005; Maïga et al., 2006), has been found to severely underestimate the nanofluid viscosity (Maïga et al., 2005).

3. Experimental apparatus and procedures

3.1. Description of the instruments and apparatus

The experimental apparatus is composed of three main components: a viscometer, its electronic control module, and a heating jacket that heats the sensor (Fig. 1a and b). The viscometer, purchased from a commercial source (ViscoLab450 Viscometer from Cambridge Applied Systems, Massachusetts, USA), uses the so-called 'piston-type' technology (Fig. 1c) in which the determination of the fluid sample viscosity is based on the Couette flow inside a cylindrical chamber. It is composed of two magnetic coils installed inside a 316 stainless steel sensor body. These coils are used to generate a magnetically-induced force on a cylindrical piston that moves back and forth over a distance of 5 mm. By alternatively powering the coils with a constant force, the elapsed time corresponding to a round trip of the piston can then be measured. This measurement is accurately related to the viscosity of the fluid sample contained in the chamber through a precise calibration process. As the piston is pulled toward the bottom of the measurement chamber, it forces the fluid at the bottom to flow around the piston toward the sensor opening. On the other hand, on the upward piston stroke, fresh fluid is pulled around the piston to thoroughly mix the contents of the measurement chamber. Such a mixing effect ensures the uniformity of fluid temperature inside the chamber. Also, since measurement of the piston motion is in two directions, variations due to gravity or flow forces are annulled. Furthermore, because of the very small mass of the piston, the induced magnetic forces greatly exceed any disturbances due to vibrations. Since the fluid viscosity may significantly vary with temperature, it is important to know the exact temperature of the measurement chamber. The temperature of the fluid sample inside the sensor chamber is therefore continuously monitored using a precision Platinum RTD that is internally mounted at the base of the chamber. The viscometer system was factory calibrated and delivered ready for operation. The temperature accuracy and repeatability of the RTD probe are estimated to be ±0.2 °C and ±0.1 °C, while the viscometer accuracy and repeatability are, respectively, ±1% and ±0.8% for the range of 0–20 cP, according to the manufacturer.

The heating jacket (Fig. 1b) consists of a solid steel cylinder of 70 cm in length, 10 cm outside diameter and 6 cm inside diameter (identical to the outside diameter of the viscometer sensor chamber). It is electrically heated by means

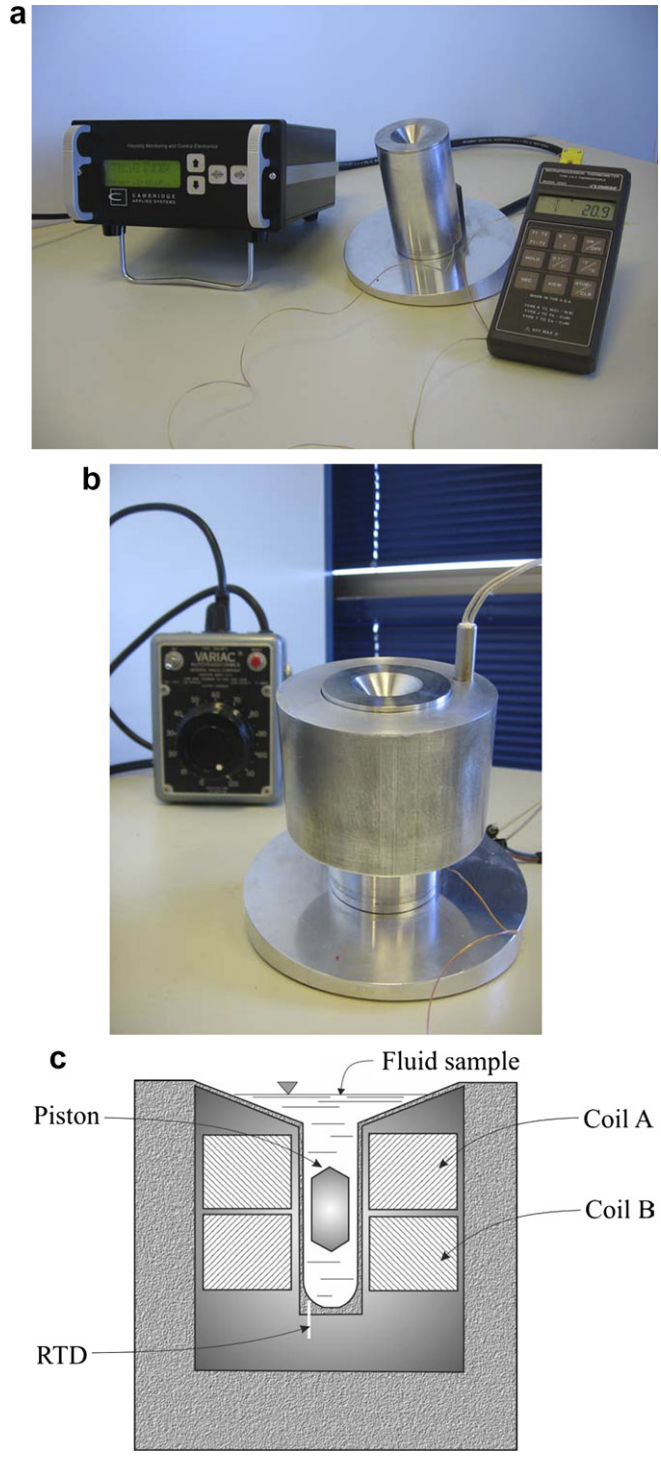

Fig. 1. (a) ViscoLab450 and controller module, (b) heating jacket with potentiometer, (c) illustration of the viscometer measurement chamber.

of a standard 50 W nominal power cartridge heater that is axially embodied inside the jacket; this heating cartridge was coupled to a standard Variac in order to modulate, if necessary, the electrical input voltage to the cartridge heater. During the heating phase, extreme precaution was exercised in order to maintain the maximum temperature of the viscometer sensor around 85 °C as recommended by the manufacturer to avoid any possible damages to the instruments and their internal wiring.

3.2. Preparation of nanofluids and experimental procedure

In the present study, we are primarily interested in establishing a viscosity database for two particular types of water-based nanofluids, namely the Al_2O_3–water nanofluid with two different average particle diameters, 36 nm and 47 nm, and the CuO–water nanofluid with 29 nm average size particles. All three mixtures have been purchased readily prepared and mixed from a commercial source (Nanophase Technologies, USA). At delivery, the original particle volume fractions were approximately 22%, 15% and 14%, respectively, for the above named mixtures. In order to produce other solutions at desired particle concentrations, dilution with distilled water followed by a stirring action was found to be quite sufficient. It should be noted that because of the application of chemical dispersants (unfortunately, no information regarding these dispersants were available from the manufacturer) the suspension stability of nanoparticles within the base fluid, distilled water, was found to be very good even after a relatively long resting period, e.g. weeks to months. After longer resting periods, a vigorous stirring action was normally sufficient to properly re-establish the particle suspension. Several particle volume fractions, ranging from 1% to a value as high as 12%, have been considered.

The experimental procedure is relatively simple. At the beginning of an experiment the mixture of a desired particle concentration is prepared, the sensor piston is removed from the measurement chamber using a magnetic pen, and the chamber is half filled with fluid. Next, the piston is transferred into the chamber, pushed downward, and the measurement chamber is then filled with the fluid sample. It is interesting to mention that the total volume of fluid sample required is only about 10 ml. With the steel jacket mounted on the outside of the sensor, the heating circuit and the viscometer controller module are added. A reading can then be taken when the viscosity/temperature data have stabilized, which can be ascertained through the % of variation of these quantities displayed on the controller panel. For a typical experiment, while using the full power of the cartridge heater (50 W), the duration of the heating phase necessary to raise the fluid sample temperature from the ambient condition to almost 80 °C was found to be approximately 4 h. In conjunction with a very low mass of the fluid sample, such a long heating duration ensured a sufficiently low thermal gradient and minimized any lag between temperature reading and viscosity measurement. Because of the long elapsed time, it was necessary to mix the fluid sample inside the measurement chamber at regular time intervals using the 'purging feature' (rapid strokes of the piston inside the measurement chamber) available on the viscometer. Tightly wrapped plastic was applied around the measuring chamber in order to reduce the

effects, if any, of water evaporation especially under elevated temperatures. This solution appeared satisfactory.

In the present study, we were also interested to determine whether there exists some hystereris behaviour on particle suspension quality due to the heating process. To do this, after reaching the desired maximum temperature, the heating power is cut off and the system is allowed to cool by natural convection toward the ambient air. During this cooling phase, which is extremely slow (it generally takes around 5 h to return to the ambient temperature) readings of fluid temperature and viscosity were continuously taken using a purging action at regular intervals.

3.3. Results from validation tests of instruments

In order to verify the precision of the ViscoLab450 viscometer as well as to assess the reliability of the experimental procedures described above, we have carried out two different sets of viscosity measurements. The first set was conducted using the CAS calibration fluid (a mineral oil with code name S3S) supplied by the manufacturer for which viscosity data are available. For the second set of tests, distilled water was used. For both fluids, values of viscosities were collected during the heating as well as the cooling phase. Fig. 2a shows that the measured viscosity values of the mineral oil are quite close to those of the manufacturer (note that non-regular intervals are used for the x-axis). In fact, the relative errors of the measured data did not exceed 3% over the temperature range tested, from 20 °C to 45 °C. Unfortunately, due to the lack of manufacturer's data, such a comparison was not possible for temperatures lower than 20 °C. For the case of distilled water we have compared the measured data to the corresponding values computed by the following correlation (Hagen, 1999):

$$\mu_{bf} \times 10^4 = \exp\left[\frac{1.12646 - 0.039638 \cdot (T + 273.15)}{1 - 0.00729769 \cdot (T + 273.15)}\right] \quad (7)$$

where T, in °C, is the fluid temperature. Fig. 2b clearly shows that the ViscoLab450 Viscometer performs quite satisfactorily in this case also. The relative errors do not exceed 6.5%, a value that is very acceptable in conjunction with experimental uncertainties. From the results of these validation tests, we are confident that not only did the viscometer perform satisfactorily, but also that the experimental procedure, in particular the heating/cooling processes of the viscometer, are appropriate for the tasks demanded.

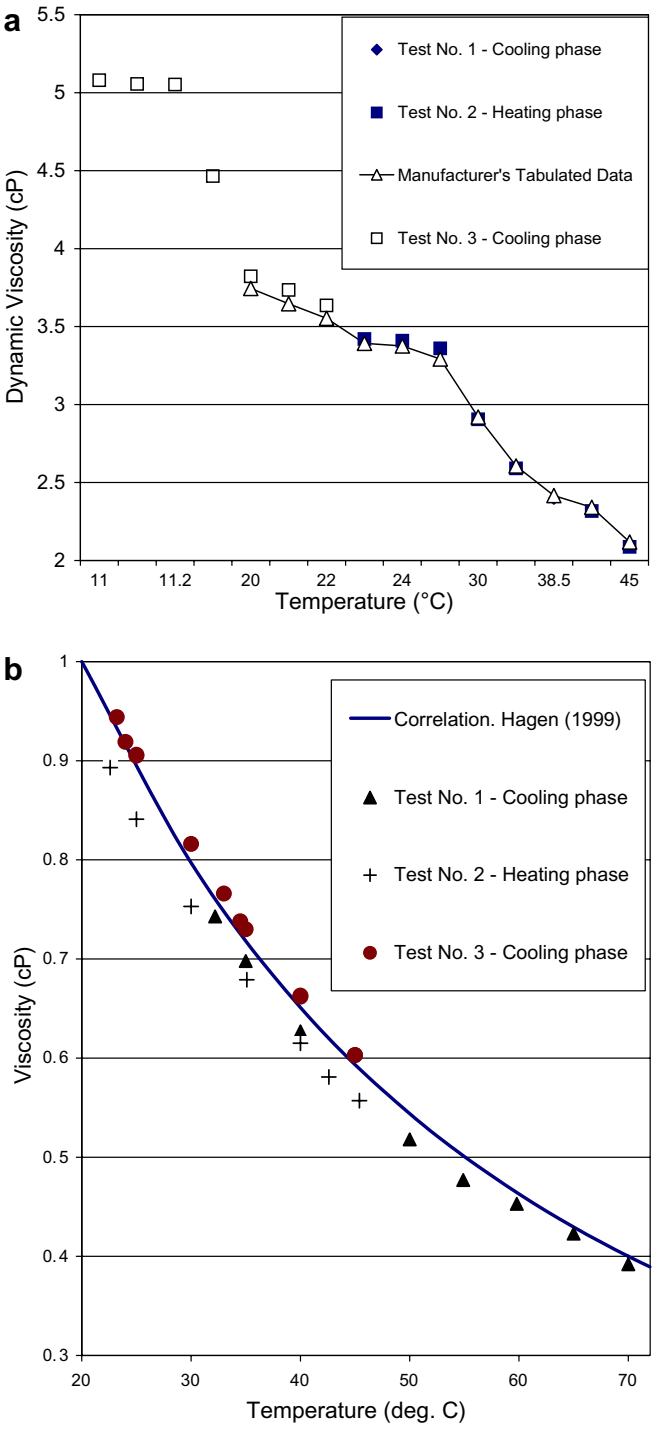

Fig. 2. Results from validation tests: (a) S3S calibration oil, (b) distilled water.

4. Presentation of viscosity data

4.1. Nanofluids viscosities at ambient temperature

Figs. 3 and 4 show viscosity data for Al_2O_3–water and CuO–water nanofluids for room condition (i.e., temperatures of fluid sample between 22 °C and 25 °C) and the particle volume fraction varying from 0.15% to as high as 13%. The results are expressed under the usual form of the viscosity as well as relative viscosity (defined as the 'nanofluid-to-water' ratio of viscosities). It is important to recall that based on the results from the validation tests using calibration fluid and distilled water one can expect maximum relative errors below 6.5% for the measured viscosities. Some limited data from other researchers are also displayed in Fig. 4 for discussion purposes. As expected,

nanofluid viscosity increases with an augmentation of particle volume fraction. Thus for 47 nm alumina–water nanofluid for example, the relative viscosity increased from nearly 1.12 to ≈1.6, to 3.0 and then to ≈5.3 for particle concentration increasing from 1% to 4%, to 9% and then to 12%. Similar behaviour was also found for the 36 nm Al_2O_3 particle size: the relative viscosity increased from ≈1.1 to ≈1.4, then to ≈2.0 and finally to ≈3.1 for particle concentration varying from 2.1% to 4.3%, to 8.5% and then to 12.2%. It is interesting to observe that viscosities of nanofluids with 36 nm particle-size are clearly lower than those with 47 nm particles. Such differences become more pronounced for particle volume fractions higher than 5%. Another point of interest is that data in Fig. 4 eloquently show that both the Brinkman (1952) and Batchelor (1977) formulas severely underestimate nanofluid viscosities, except at very low particle volume fractions. Such result is discussed in detail in Section 4.3. Furthermore, while attempting to compare our measured data to those from other researchers, an apparently contradictory behaviour has been noticed regarding the effect of particle size. Pak and Cho (1998) data obtained for 13 nm particle-size are much higher than all other results while Wang et al. (1999) data fall relatively close to ours. In our opinion, it is difficult to draw any conclusive remarks about such result, except to say that this intriguing behaviour may be attributed to various factors such as nanofluid preparation methods. This is, in fact, one of the major concerns in nanofluid studies (Keblinski et al., 2005). For computing purpose, we have proposed the following correlations for the Al_2O_3–water nanofluids tested:

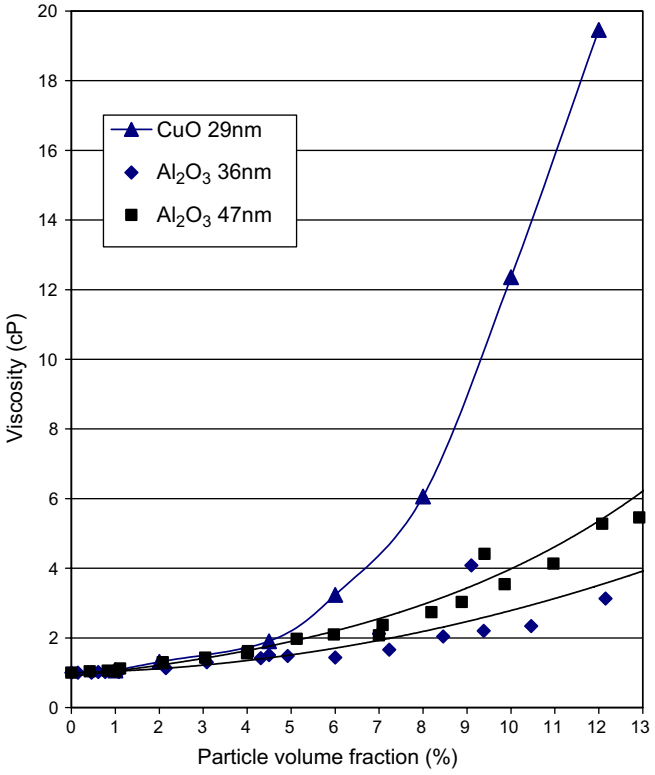

Fig. 3. Viscosity data at ambient temperature for nanofluids considered.

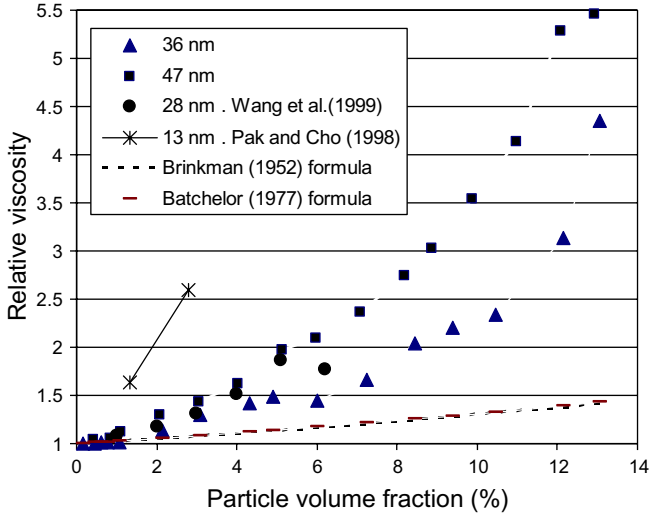

Fig. 4. Water–Al_2O_3 relative viscosity from various sources (ambient condition).

$$\mu_r = \frac{\mu_{nf}}{\mu_{bf}} = 0.904e^{0.148\cdot\varphi} \tag{8}$$

for 47 nm particle-size, and:

$$\mu_r = 1 + 0.025\varphi + 0.015\varphi^2 \tag{9}$$

for 36 nm size.

For CuO–water nanofluid under ambient condition, similar behaviour regarding the viscosity increase with respect to particle fraction was also found, Fig. 3. It is very interesting to observe that for particle volume fractions lower than 4%, the viscosity of CuO–water is almost the same as that of the alumina–water nanofluids considered earlier. However, for higher particle loading, the increase in viscosity with respect to particle concentration is clearly much greater. Such high values of viscosity may result from the intrinsic molecular structure of the mixture itself and the particular chemical dispersing agents used. Also, we can see that the use of the Batchelor (1977) and Brinkman (1952) formulas for CuO–water nanofluid is inappropriate. Therefore, we have proposed the following correlation for computing CuO–water viscosity:

$$\mu_r = 1.475 - 0.319\varphi + 0.051\varphi^2 + 0.009\varphi^3 \tag{10}$$

4.2. Nanofluid viscosity data function of temperature

We measured extensively viscosities for the three nanofluids considered for particle volume fraction ranging from 1% to nearly 9.4% and for temperatures varying from room condition to 75 °C approximately. In total, almost five hundred data points were collected for both distilled water and nanofluids. It is worth noting that for alumina–water nanofluid, most of these data have been collected from dif-

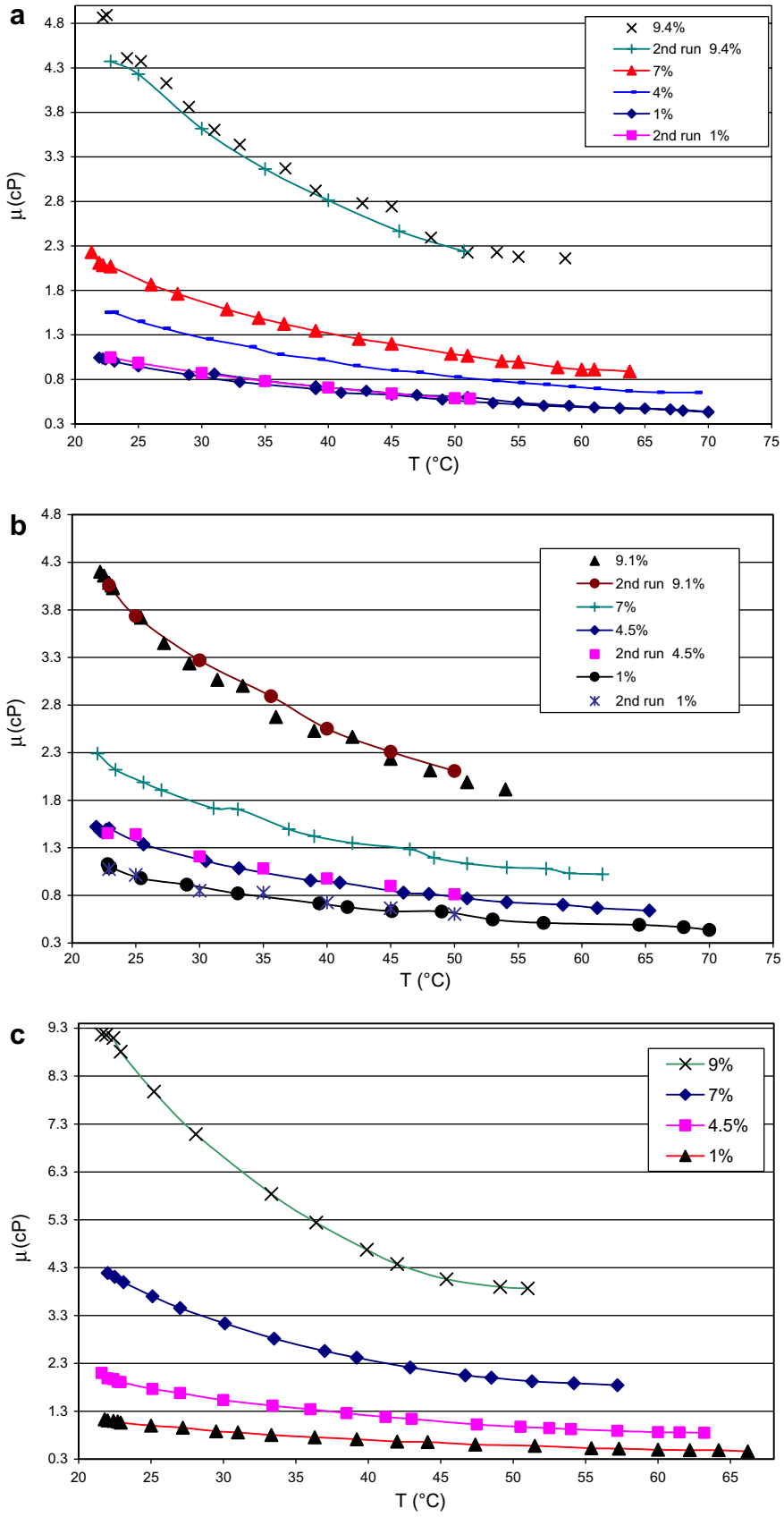

Fig. 5. Viscosity data for: (a) water–Al_2O_3 – 47 nm, (b) water–Al_2O_3 – 36 nm and (c) water–CuO – 29 nm.

ferent runs using new fluid samples in order to ensure not only the consistence but also the repeatability of data. The complete data base is shown in Fig. 5a and b for alumina–water with 47 nm and 36 nm and in Fig. 5c for CuO–water; while the corresponding least-square fitting curves are shown in Fig. 6a–c.

It can be observed that in general, nanofluid viscosity increases considerably with increasing particle volume frac-

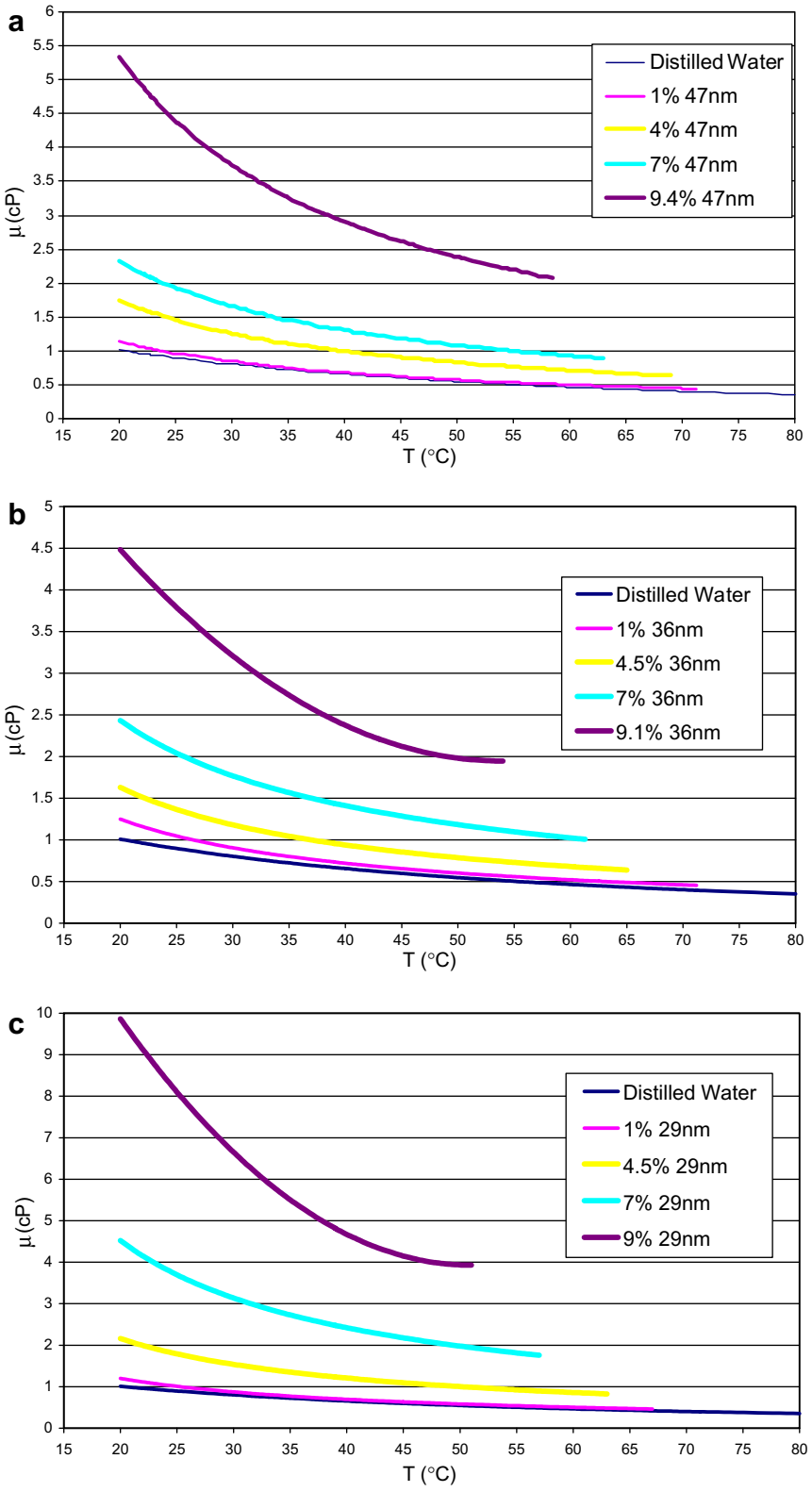

Fig. 6. Viscosity curves for: (a) water–Al_2O_3 – 47 nm, (b) water–Al_2O_3 – 36 nm and (c) water–CuO – 29 nm.

tion, but decreases with an augmentation in temperature. The first effect is due to the fact that increasing concentration would have a direct effect on the fluid internal shear stress while the temperature effect is obviously due to a weakening of inter-particle and inter-molecular adhesion forces. Thus, for water–Al_2O_3 and 47 nm particle-size in particular, viscosities for 30 °C are approximately 0.8, 1.3, 1.7 and 3.6cP, for concentrations of 1%, 4%, 7% and 9.4%, respectively. Similar behaviours were found for 36 nm alumina–water as well as for 29 nm CuO–water. For the latter, viscosities are generally much higher than those of alumina–water nanofluids, especially for high particle concentrations; thus, for 30 °C for example, CuO–water viscosities are 0.9, 1.5, 3.1 and 6.5cP for particle concentrations of 1%, 4.5%, 7% and 9%, respectively. It is also interesting to note that for all the nanofluids tested, the temperature gradient of viscosities is generally more important for temperatures around ambience, e.g. from 22 °C to 40 °C. Such viscosity gradient is particularly more pronounced for high particle fraction, for example for 9%. This result suggests that temperature effects on particle suspension properties may be very different for high particle fraction than for lower ones. With an increase of temperature, measured viscosity data have shown a certain asymptotic behaviour, i.e., viscosities tend to become almost constant regardless of temperature. In fact, for given nanofluid and particle fraction, we have observed that there exists a critical temperature, T_{cr}, beyond which irreversible damage seems to be done to the particle suspension properties, which, in turn, produces an unexplainable and somewhat 'erratic' increase of nanofluid viscosity. The hysteresis phenomenon, which will be described and discussed in details later in Section 4.4, has clearly been observed when heating the fluid sample beyond T_{cr}. Such intriguing behaviour remains not completely understood, and more data is needed. At present, we can state only that this T_{cr} seems to be strongly dependent not only on particle concentration but also on particle-size (Table 1). T_{cr} corresponds to the last points on the data curves shown in Fig. 5a–c.

Fig. 6a–c illustrate the tendency curves obtained by curve-fitting of the data collected. It is worth noting that for each of the figures, the lowest curve corresponds to distilled water viscosity as given by Eq. (7), while the other curves, from the lowest to the highest, correspond to the four different particle concentrations considered. The previously discussed behaviours regarding the effects due to temperature as well as to particle volume fraction can be clearly observed in these figures. T_{cr} corresponds to the highest temperature at the end of each curve.

Table 1
Effect of particle size on T_{cr} (°C) for nanofluids considered

	Al_2O_3		CuO
	47 nm	36 nm	29 nm
1%	N/A[a]	N/A[a]	66.2
4%	69	65.3	63.2
7%	63.8	61.6	57.2
9%	58.7	54	51

[a] Hysteresis phenomenon not observed for the temperature range considered.

As previously stated, data obtained for the considered nanofluids, in particular those for Al_2O_3–water mixture with high particle concentrations as well as those for CuO–water nanofluid, are believed to be the first of their kind. For Al_2O_3–water in particular, although there exist some data by Maré et al. (2006) and Masuda et al. (1993), it appears difficult to draw any conclusive comparisons. In fact, from data shown in Fig. 7 for the particular case of alumina–water mixture with particle volume fraction of ≈4.5%, we can observe that while there seems to be negligible difference in our viscosity data for both 36 nm and 47 nm particle-sizes, those by Masuda et al. (1993) for 13 nm size are clearly higher than ours. On the other hand, Maré et al. (2006) considered 47 nm particle-size and, using a Brookfield-rotating-cylinder viscometer, obtained a very different scale of viscosity: their data are three times higher than ours, in spite of all the precautions taken. This result indicates that data for nanofluid properties may differ significantly from one source to another. We believe that such a discrepancy is due mainly to the differences of preparation methods used for synthesizing nanofluids (see in particular Keblinski et al., 2005; Eastman et al., 2004).

4.3. Nanofluid relative viscosity as function of temperature

In the present study, we are also interested to determine whether Einstein's formula and the other expressions presented in Section 2 can be used to represent temperature-dependent viscosities for the nanofluids tested. Fig. 8a and b shows, respectively, for Al_2O_3–water and CuO–water nanofluids, the results for the relative viscosity as a function of temperature. It is interesting to observe that for particle concentrations lower than 4%, all tested nanofluids exhibit almost constant relative viscosities that are independent of temperature. Between the two alumina–water nanofluids, there are only slight differences in the levels of relative viscosity. Such differences however become much more visible for higher particle fraction, e.g. for 7% and 9% (Fig. 8a), where we can observe not only a temperature-dependence, but a particle-size-dependence as well. The effect due to particle-size appears somewhat paradoxical: for a particle fraction of 7% for example, viscosities for 36 nm are slightly higher than those of 47 nm; while for a 9% volume fraction, the reverse behaviour is found. With regard to a water–CuO mixture, similar behaviours have also been found, although levels of relative viscosity are much higher than those observed for alumina–water nanofluids. Thus, for a 9% volume fraction for example, relative viscosities of CuO–water range from 7 to almost 10, i.e., 7–10 times the viscosities of water. Such a high level of viscosity may impose severe restrictions on the use of nanofluids in practical thermal applications.

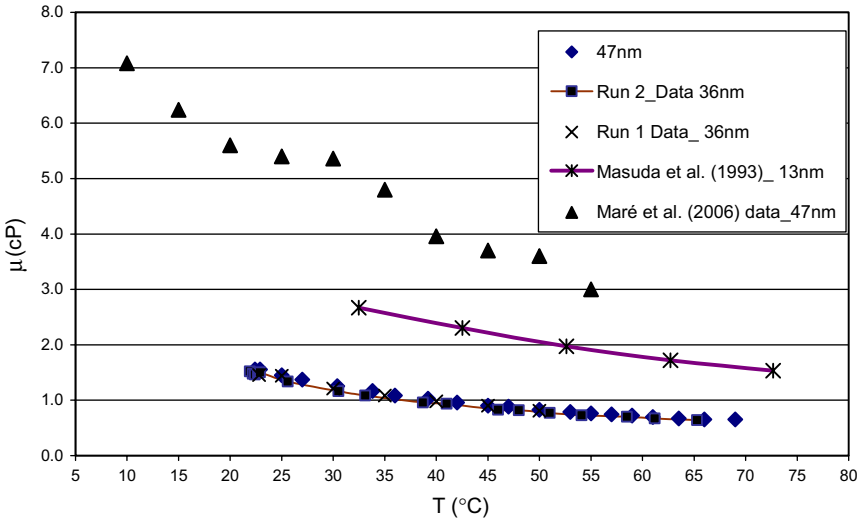

Fig. 7. Other viscosity data for water–Al_2O_3 (≈4.5% particle concentration).

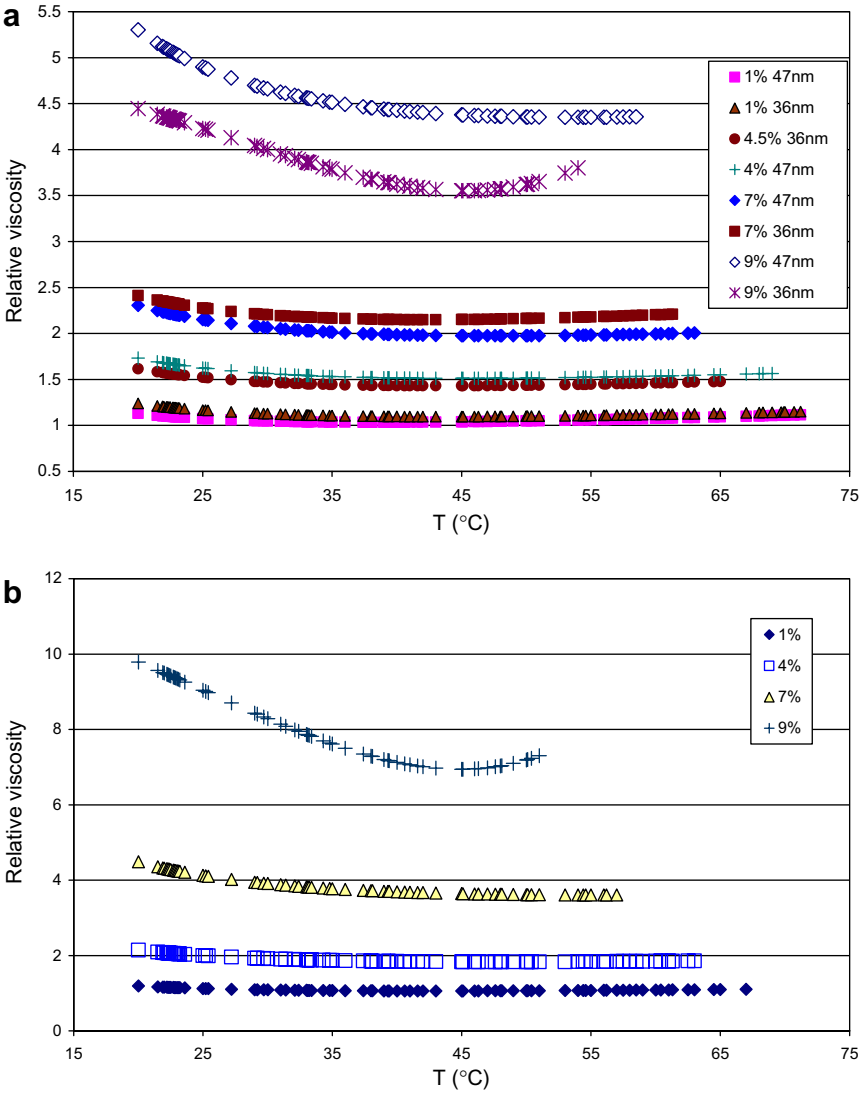

Fig. 8. Relative viscosity data for water–Al_2O_3 and water–CuO nanofluids.

From the above temperature and particle-size dependence of relative viscosities, we found that none of the formulas cited in Section 2 would be applicable for the nanofluids studied, especially for particle concentrations higher than 4%. In fact, even for low particle concentrations, e.g. 1% and 4%, Einstein's formula as well as those of Brinkman (1952), Lundgren (1972), Batchelor (1977) and Graham (1981) have, as we may expect, underestimated nanofluids viscosities. Thus, for a 1% particle fraction, these formulas give values of 1.025–1.026 for relative viscosity, while our data give values of 1.05–1.29 for Al_2O_3–water and 1.05–1.19 for CuO–water. For a 4% concentration in particular, relative viscosities range from 1.1 to 1.11 according to these formulas, which are drastically underestimated with respect to our data, namely 1.43–1.73 for Al_2O_3–water and 1.83–2.14 for CuO–water. This result, similar to that observed earlier for viscosity data at ambient temperature (Section 4.1), may be explained by the fact that Einstein's formula, and all others originating from it, were obtained based on the theoretical assumption of a linear fluid surrounding isolated particles. Such a model may well represent the situation of a liquid that contains a small number of dispersed particles. For nanofluids in particular, this may correspond to a very low particle volume fraction, e.g. below 1%, as it seems to be corroborated by the measured data for 1% particle volume fraction. However, for higher particle concentrations the departure of these formulas from our experimental data is considerable, indicating that the linear fluid theory is no longer appropriate to represent nanofluid reality. Even Batchelor's formula (1977), the one that considered Brownian effects, performs poorly. A possible explanation of this is the fact that for the nanofluids tested in this study, the use of chemical surfactants to maintain good particle suspension properties can affect the inter-particles forces. We believe that this effect requires further investigation.

The following formulas have been proposed for computing the dynamic viscosity for all three nanofluids tested and particle concentrations of 1% and 4%, respectively:

$$\mu_{nf} = \mu_{bf}(1.1250 - 0.0007 \cdot T) \quad (11)$$

$$\mu_{nf} = \mu_{bf}(2.1275 - 0.0215 \cdot T + 0.0002 \cdot T^2) \quad (12)$$

where T is temperature in °C (it is obvious that because of the particular form of these equations, the coefficients preceding the variables T and T^2 have, as unit, $°C^{-1}$ and $°C^{-2}$, respectively). On the relative error basis, the correlations (11) and (12) exhibit average errors of 0.06% and 1.28%, and standard-deviations of 3.75% and 11.39%, respectively. These values are considered acceptable in conjunction with experimental uncertainties. Unfortunately, for higher particle volume fractions, it was not possible to provide any correlations that could take into consideration the combined effects due to temperature, particle concentration and size.

4.4. Hysteresis phenomenon on viscosity measurement

As mentioned, our observations and experimental data have clearly revealed the existence of a critical temperature beyond which nanofluid viscous behaviour becomes drastically altered. Specifically, it has been found that for intermediate to high particle concentrations, a large increase of viscosity is observed when a fluid sample is heated beyond a critical temperature. And if the fluid sample is subsequently cooled, a hysteresis on viscosity measurement occurs. This rather intriguing phenomenon may be better understood by scrutinizing Fig. 9a that shows viscosity data obtained for Al_2O_3–water with 47 nm particle-size and 7% particle volume fraction during experiments of heating and cooling. We first performed Run 1, 'heating phase', which was followed by Run 1a, 'cooling phase'. Data collected in Run 1 showed that at 61.3 °C approximately, nanofluid viscosity reached its lowest level. Beyond this temperature the viscosity increases with increasing temperature. This behaviour has been confirmed by performing another run, Run 2 'heating phase'. We note the low data dispersion between Runs 1 and 2, which proves the consistency and reliability of the instruments used and of the experimental procedures adopted. When the fluid sample was heated beyond 61.3 °C and then cooled slowly, a hysteresis behaviour was clearly observed. Thus, during the cooling operations (Runs 1a and 2a) measured viscosities at any given temperature are considerably higher than those measured during the heating phases (Runs 1 and 2). One may conclude that for Runs 1a and 2a, some irreversible damage has occurred to the particle suspension properties. It is interesting to note that the only difference between Runs 1a and 2a is in level of the highest temperature reached by the fluid sample prior to cooling. These temperatures are approximately 69 °C for Run 1a and 71.2 °C for Run 2a. One can also observe from Fig. 9a that viscosities of Run 2a are clearly higher that those of Run 1a, which gives the indication that damage to particle suspension properties is more pronounced in Run 2a than in Run 1a. Thus, the temperature level which the fluid sample reaches during a heating phase is of crucial importance with regard to possible damages done to the nanofluid rheological properties. It is worth noting that if the heating of the fluid sample stops below the critical temperature, T_{cr} no hysteresis takes place during cooling.

This interesting phenomenon was also observed for 36 nm particle-size Al_2O_3–water (Fig. 9b) and 29 nm particle-size CuO–water (Fig. 9c). It is interesting to observe that for a low particle fraction, e.g. 1%, we detected no sign of hysteresis for either 47 nm or 36 nm particle-sizes. However, for higher particle loading, hysteresis does exist, becoming more pronounced with an increase of particle fraction. For Al_2O_3–water – 36 nm and concentrations of 7% and 9% (Fig. 9b), the hysteresis observed was particularly severe, especially for the 9% particle fraction for which the heating phase beyond the critical temperature was stopped short as fluid sample became very sticky. This

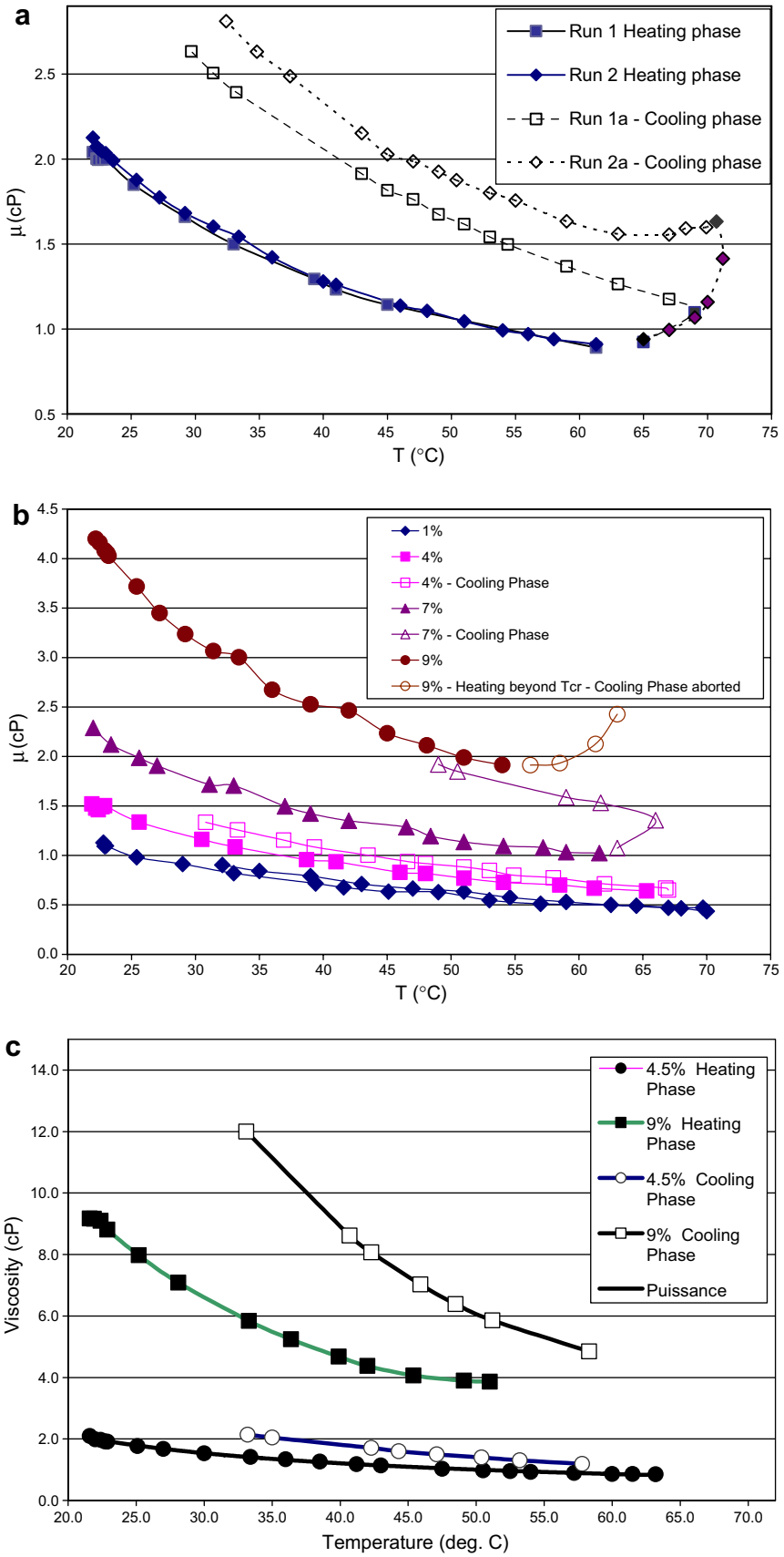

Fig. 9. Hysteresis observed on viscosity measurements for: (a) water–Al_2O_3 – 47 nm (7%), (b) water–Al_2O_3 – 36 nm and (c) water–CuO – 29 nm.

indicates a rather drastic alteration of nanofluid rheological properties. Fig. 9c shows a similar hysteresis phenomenon for 29 nm CuO–water and specific particle volume fractions of 4.5% and 9%. Here again, the hysteresis is rather severe: for the 9% particle volume fraction in particular, the levels of viscosity measured during the cooling phase are almost twice those of the heating phase. For this concentration, the value of T_{cr} is quite low and has been estimated at 51 °C. Table 1 presents experimental values of T_{cr} for the nanofluids under consideration. The critical temperature appears strongly dependent on both particle concentration and size: T_{cr} decreases with increasing particle fraction and, for a given particle concentration, T_{cr} decreases with decreasing particle size.

The above intriguing hysteresis is still poorly understood. We believe that a considerable increase of nanofluid viscosity during the cooling operation, e.g. Runs 1a and 2a (see again Fig. 9a), may be caused by drastic yet unknown changes that have been produced by temperature changes. In fact, visual inspection of fluid samples at the end of Runs 1a and 2a reveal a highly viscous fluid with the presence of particle agglomerates on the inner surface of the measuring chamber. This suggests that particle suspension properties have been greatly altered or, worse, destroyed when the fluid sample is heated beyond the critical temperature. This may be linked to the presence of dispersing agents, i.e., the chemical agents (often polymers) used as surfactants to maintain the particles in stable suspension. We believe that beyond a critical temperature, these surfactants are broken down and their performance is considerably reduced or even destroyed, causing the particles to lose their suspension capabilities. The particles then have a tendency to form agglomerations resulting in the observed drastic and unpredictable increase of the nanofluid viscosity. Such an argument appears, in our opinion, physically plausible. It indicates that, once the deterioration of particle suspension properties is initiated, the presence of more particles inside the base fluid (i.e., higher particle volume fractions for given particle-size or smaller particle-size for given particle volume fraction) would result in a more pronounced effect on nanofluid viscosity. This explanation is well corroborated by the experimentally determined values for T_{cr} (see again Table 1). Unfortunately, it was not possible to obtain any information regarding the nature and characteristics of the dispersing agents used by the manufacturer in order to verify these statements. More investigations are necessary in order to completely understand this hysteresis phenomenon.

4.5. Hysteresis: is heat transfer enhancement by using a nanofluid still possible?

In light of the hysteresis observed on viscosity measurement, one can wonder if it would be realistic to consider using nanofluids for heat transfer enhancement purposes, enhancement that has been acclaimed by many researchers in recent years. It must be clear at this stage that in the occurrence of a hysteresis behaviour and unpredictable increase of viscosity inside a nanofluid, the entire flow field and heat transfer behaviour would become completely unpredictable. For non-isothermal flow situations, the behaviour and development of both the flow and thermal fields, especially in the vicinity of boundary layers, would also become highly unpredictable. This situation is obviously undesirable and may seriously compromise the potential use of nanofluids in thermal applications, in spite of their interesting features.

It is worth mentioning that for some confined flow situations, it has been experimentally demonstrated that an inclusion of nanoparticles within viscous fluids produces a substantial heat transfer enhancement, see in particular Pak and Cho (1998), Li and Xuan (2002) and Nguyen et al. (2006a). In these works the hysteresis phenomenon was not observed, probably because of the relatively low temperatures considered, i.e., below the critical temperatures. It is also possible that the presence of a strong forced convection flow has attenuated the effects, if any, resulting from a hysteresis phenomenon. Thus, the heat transfer enhancement capabilities of nanofluids for cases of forced convection flows are really present, and this, despite the fact that the physical mechanisms behind such enhancement have yet been completely understood (Keblinski et al., 2005). On the other hand, it has also been found, through experimental observations and data, that high temperature levels may drastically alter or even destroy particle suspension properties, which, in turn, has a direct impact on heat transfer. In particular, Putra et al. (2003) and Nguyen et al. (2006b) have observed that for cases of natural convection in an enclosure and pool boiling using Al_2O_3–water nanofluids, such alteration of particle suspension properties was responsible of the deterioration of the surface heat transfer coefficient.

In summary, one can believe with confidence that the nanofluids constitute an interesting alternative for various thermal applications, their use, however, from the practical viewpoint, seems to be limited for low temperatures. The obvious question is then how to produce a 'suitable' nanofluid to accomplish the goal of heat transfer enhancement. More precisely, in light of the hysteresis phenomenon observed in this work, nanofluids must possess indeed stable particle suspension properties over wide ranges of temperature. Such a formidable task represents an interesting challenge from the manufacturing viewpoint as particle suspension properties seem to be closely influenced not only by properties of the constituents used but also by the methods employed to produce the suspensions themselves.

5. Conclusion

In this paper, we have established a new and more complete viscosity data base for two particular water-based nanofluids, namely water–Al_2O_3 with 36 nm and 47 nm particle-sizes and water–CuO with 29 nm particle-size.

Using a 'piston-type' calibrated viscometer combined with a cylindrical and heated chamber, data were first collected for ambient condition and particle volume fractions up to almost 12%. The effects due to temperature and particle-size were investigated for fluid temperatures ranging from 22 °C to 75 °C and particle volume fractions varying from 1% to 9.4%. For all the nanofluids tested, their viscosities were found to be strongly dependent on both temperature and particle volume fraction. In general, the dynamic viscosity of nanofluid increases with an augmentation of particle volume fraction (for a given temperature), but decreases with increasing temperature (for a given particle concentration). For water–alumina nanofluid, it was observed that particle-size effects are more important for high particle concentrations. Similar behaviours were found for a CuO–water mixture regarding the effects due to temperature and particle concentration, although its viscosity levels are generally much higher than those of Al_2O_3–water. Several correlations were proposed for computing nanofluids viscosities for low particle concentrations. Experimental data have clearly revealed the existence of critical temperatures beyond which the hysteresis phenomenon occurs. This hysteresis, which is believed to be the first observed for nanofluids, has raised serious concerns regarding the use of nanofluids for heat transfer enhancement purposes. Finally, it has been found that Einstein's formula and several others originating from the linear fluid theory seem not to be applicable for the nanofluids tested, especially for intermediate to high particle volume fractions.

Acknowledgements

The authors thank the *Natural Sciences and Engineering Research Council of Canada* and the Faculty of the Graduate Studies and Research of the *Université de Moncton* for financial support for the present project, and to the *Institut Supérieur de Technologie Midi-Pyrénées* and *Pierre Fabre Medicament Production (France)* for making possible an internship to Mr. Franck Desgranges. Our sincere thanks are also to Mrs. Vivienne Galanis for reading and improving the revised text.

References

Batchelor, G.K., 1977. The effect of Brownian motion on the bulk stress in a suspension of spherical particles. J. Fluid Mech. 83 (1), 97–117.

Ben Mansour, R., Galanis, N., Nguyen, C.T., 2006. Developing laminar mixed convection of nanofluids in a horizontal tube with uniform wall heat flux. In: Proceedings of the 13th IHTC, 13–18 August 2006, Sydney, Australia.

Ben Mansour, R., Galanis, N., Nguyen, C.T., 2007. Effect of uncertainties in physical properties on forced heat transfer with nanofluids. Appl. Therm. Eng. 27 (1), 240–249.

Brinkman, H.C., 1952. The viscosity of concentrated suspensions and solution. J. Chem. Phys. 20, 571–581.

Chein, R., Huang, G., 2005. Analysis of microchannel heat sink performance using nanofluids. Appl. Therm. Eng. 25, 3104–3114.

Choi, S.U.S., 1995. Enhancing Thermal Conductivity of Fluids with Nanoparticles. ASME Publications FED-Vol. 231/MD-Vol. 66, pp. 99–105.

Chon, C.H., Kilm, K.D., Lee, S.P., Choi, S.U.S., 2005. Empirical correlation finding the role of temperature and particle size for nanofluid (Al_2O_3) thermal conductivity enhancement. Appl. Phys. Lett. 87, 153107-1–153107-3.

Das, S.K., Putra, N., Thiesen, P., Roetzel, W., 2003. Temperature dependence of thermal conductivity enhancement for nanofluids. J. Heat Transfer 125, 567–574.

Daungthongsuk, W., Wongwises, S., 2007. A critical review of convective heat transfer of nanofluids. Renew. Sust. Energ. Rev. 11 (5), 797–817.

Eastman, J.A., Choi, S.U.S., Li, S., Soyez, G., Thompson, L.J., DiMelfi, R.J., 1999. Novel thermal properties of nanostructured materials. J. Metastable Nanocryst. Mater. 2 (6), 629–634.

Eastman, J.A., Choi, S.U.S., Li, S., Yu, W., Thompson, L.J., 2001. Anormalously increase effective thermal conductivities of ethylene glycol-based nanofluids containing copper nanoparticles. Appl. Phys. Lett. 78 (6), 718–720.

Eastman, J.A., Phillpot, S.R., Choi, S.U.S., Keblinski, P., 2004. Thermal transport in nanofluids. Annu. Rev. Mater. Res. 34, 219–246.

Einstein, A., 1906. Eine neue Bestimmung der Moleküldimensionen. Annalen der Physik 19, 289–306.

Frankel, N.A., Acrivos, A., 1967. On the viscosity of a concentrate suspension of solid spheres. Chem. Eng. Sci. 22, 847–853.

Graham, A.L., 1981. On the viscosity of suspensions of solid spheres. Appl. Sci. Res. 37, 275–286.

Hagen, K.D., 1999. Heat Transfer with Applications. Prentice-Hall, New Jersey, USA, pp. 637–638.

Keblinski, P., Eastman, J.A., Cahill, D.G., 2005. Nanofluids for thermal transport, Materials today, June 2005 Issue, pp. 36–44.

Koo, J., Kleinstreuer, C., 2005. A new thermal conductivity model for nanofluids. J. Nanoparticle Res. 6, 577–588.

Lee, S., Choi, S.U.S., 1996. Application of metallic nanoparticle suspensions in advanced cooling systems, ASME Publications PVP-Vol. 342/MD-Vol. 72, pp. 227–234.

Lee, S., Choi, S.U.S., Li, S., Eastman, J.A., 1999. Measuring thermal conductivity of fluids containing oxide nanoparticles. J. Heat Transfer 121, 280–289.

Li, Q., Xuan, Y., 2002. Convective heat transfer performances of fluids with nano-particles. In: Proceedings of the 12th International Heat Transfer Conference, Grenoble, France, pp. 483–488.

Liu, M.S., Lin, M.C.-C., Huang, I.-Te., Wang, C.-C., 2006. Enhancement of thermal conductivity with CuO for nanofluids. Chem. Eng. Technol. 29 (1), 72–77.

Lundgren, T.S., 1972. Slow flow through stationary random beds and suspensions of spheres. J. Fluid Mech. 51, 273–299.

Maïga, S.E.B., Palm, S.J., Nguyen, C.T., Roy, G., Galanis, N., 2005. Heat transfer enhancement by using nanofluids in forced convection flows. Int. J. Heat Fluid Flow 26, 530–546.

Maïga, S.E.B., Nguyen, C.T., Galanis, N., Roy, G., Maré, T., Coqueux, M., 2006. Heat transfer enhancement in turbulent tube flow using Al_2O_3 nanoparticle suspension. In: Lewis, R.W., (Eds.), Int. J. Num. Meth. Heat Fluid Flow, vol. 16(3), pp. 275–292.

Maré, T., Schmitt, A.-G., Nguyen, C.T., Miriel, J., Roy, G., 2006. Experimental heat transfer and viscosity study of nanofluids: water–γAl_2O_3. In: Proceedings of the 2nd International Conference on Thermal Engineering Theory and Applications, Paper No. 93, January 3–6, 2006, Al Ain, United Arab Emirates.

Masuda, H., Ebata, A., Teramae, K., Hishinuma, N., 1993. Alteration of thermal conductivity and viscosity of liquid by dispersing ultra-fine particles (dispersion of γ-Al_2O_3, SiO_2 and TiO_2 ultra-fine particles). Netsu Bussei 4 (4), 227–233 (in Japanese).

Murshed, S.M.S., Leong, K.C., Yang, C., 2005. Enhanced thermal conductivity of TiO_2–water based nanofluids. Int. J. Thermal Sci. 44, 367–373.

Nanophase Technologies, <www.nanophase.com>.

Nguyen, C.T., Roy, G., Suiro, S., Maré, T., Galanis, N., 2006a. Experimental investigation of heat transfer enhancement by using a nanofluid for electronic cooling system. In: Proceedings of the 13th IHTC, 13–18 August 2006, Sydney, Australia.

Nguyen, C.T., Galanis, N., Roy, G., Divoux, S., Gilbert, D., 2006b. Pool boiling characteristics of water–Al_2O_3 nanofluid. In: Proceedings of the 13th IHTC, 13–18 August 2006, Sydney, Australia.

Pak, B.C., Cho, Y.I., 1998. Hydrodynamic and heat transfer study of dispersed fluids with submicron metallic oxide particles. Exp. Heat Transfer 11 (2), 151–170.

Palm, S.J., Roy, G., Nguyen, C.T., 2004. Heat transfer enhancement in a radial flow cooling system using nanofluids. In: Proceedings of the CHT-04 ICHMT International Symposium Advances Computational Heat Transfer, April 19–24 Norway, Paper No. CHT-04-121, 18p.

Polidori, G., Fohanno, S., Nguyen, C.T., in press. A note on heat transfer modeling of Newtonian nanofluids. Int. J. Therm. Sci.

Putra, N., Roetzel, W., Das, S.K., 2003. Natural convection of nanofluids. Heat Mass Transfer 39, 775–784.

Roy, G., Nguyen, C.T., Comeau, M., 2006a. Electronic component cooling enhancement using nanofluid in a radial flow cooling system. J. Enhanced Heat Transfer 13 (2), 101–115.

Roy, G., Nguyen, C.T., Doucet, D., Suiro, S., Maré, T., 2006b. Temperature dependent thermal conductivity evaluation of Alumina based nanofluids. In: Proceedings of the 13th IHTC, 13–18 August 2006, Sydney, Australia.

Wang, X., Xu, X., Choi, S.U.S., 1999. Thermal conductivity of nanoparticles–fluid mixture. J. Thermophys. Heat Transfer 13 (4), 474–480.

Xie, H., Fujii, M., Zhang, X., 2005. Effect of interfacial nanolayer on the effective thermal conductivity of nanoparticle–fluid mixture. Int. J. Heat Mass Transfer 48, 2926–2932.

Xuan, Y., Li, Q., 2000. Heat transfer enhancement of nanofluids. Int. J. Heat Fluid Flow 21, 58–64.

Xuan, Y., Roetzel, W., 2000. Conceptions for heat transfer correlation of nanofluids. Int. J. Heat Mass Transfer 43, 3701–3707.

Xuan, Y., Li, Q., Hu, W., 2003. Aggregation structure and thermal conductivity of nanofluids. AIChE J. 49 (4), 1038–1043.